Limnol. Oceanogr., 43(1), 1998, 53–64

Burial efficiency of phosphorus and the geochemistry of iron in continental margin sediments

Pierre Anschutz,[1] *Shaojun Zhong,*[2] *and Bjørn Sundby*
INRS-Océanologie, Université du Québec, Rimouski, Québec G5L 3A1

Alfonso Mucci
Department of Earth and Planetary Sciences, McGill University, Montréal, Québec H3A 3A1

Charles Gobeil
Institut Maurice-Lamontagne, Ministère des Pêches et des Océans, B.P. 1000, Mont-Joli, Québec G5H 3Z4

Abstract

We have examined the distributions of phosphorus and iron in sediments from well-oxygenated environments on the Atlantic Canadian and the Portuguese continental margins and from the anoxic region of the Chesapeake Bay. The measurements include total, citrate-dithionite-bicarbonate (CDB) extractable, ascorbate extractable, and dissolved P and Fe; acid volatile sulfide; and pyrite. A surface layer (varying in thickness between 2 and 4 cm) enriched in P and Fe was revealed by both the CDB and the ascorbate extractions in all sediments except those from the Chesapeake Bay. The amount of phosphate extracted by the two reagents was similar, but more iron was extracted by the CDB reagent, probably because of its ability to dissolve crystalline iron oxides. Within the Fe- and P-enriched surface layer, the Fe:P ratio in the ascorbate extract varied within a narrow range (6–14), as did the soluble-reactive phosphate (SRP) concentration (5–16 μM), suggesting that SRP is in sorption equilibrium with the solid phase. Our data are consistent with a dynamic cycling of P and strong interactions between the cycles of P, Fe, and sulfur in many marine environments. The reductive dissolution of amorphous Fe during burial and the formation of pyrite diminish the capacity of the sediment to sequester P, and only a portion of the P that arrives at the sediment–water interface actually gets buried with the sediment.

There is much interest in the ability of sediments to sequester and bury phosphorus because of the effects on the oceanic P budget (Froelich et al. 1982; Howarth et al. 1995; Ruttenberg and Berner 1993) and on the chemistry of the ocean and the atmosphere throughout geologic time (Broecker 1982; Van Cappellen and Ingall 1996). On shorter time scales, P sequestration by sediments affects the trophic state of lakes and the productivity of estuaries (Nixon 1981; Caraco et al. 1990).

Both the amount and the form of P sequestered by sediments are affected by diagenesis. Near the sediment–water interface, where most of the freshly deposited organic matter is decomposed, phosphate is rapidly remineralized and released to the sediment pore water from which it can readily escape to the overlying water. Consequently, only a portion of the particulate P that reaches the sediment–water interface is actually buried with the accumulating sediment (Krom and Berner 1980, 1981; Balzer 1986; Sundby et al. 1992). Deeper in the sediment, organic P may be converted to apatite without loss of P from the sediment (Ruttenberg and Berner 1993). P sequestration is particularly important along the continental margins, where most terrigeneous material settles out. However, this is also where diagenesis may have the greatest effect on P burial. In the Laurentian Trough in the Gulf of St. Lawrence, for example, only half of the sedimentation flux of particulate P is buried (Sundby et al. 1992). In the shallower Aarhus Bay (Denmark), as little as 30% of the P flux is buried (Jensen et al. 1995).

The factors controlling the burial efficiency of P are not completely understood, but one important factor seems to be the adsorption capacity of the sediment for phosphate, which generally decreases rapidly with depth below the sediment surface. This decrease has been attributed to the progressive reductive dissolution of iron oxides upon burial (Krom and Berner 1980). For this reason, we have examined the distribution of several operationally defined reactive phases of both Fe and P in several different continental margin sediments. This study focuses on processes affecting P and Fe in the upper 20 cm of the sediment column, which we have sampled with high spatial resolution. We do not consider P transformations that take place deeper in the sediment.

Methods

Sediment box cores were collected at the locations indicated in Table 1. Locations include the Gulf of St. Lawrence,

[1] Present address: Université de Bordeaux I, DGO-URA 197, 33405 Talence Cedex, France.

[2] Present address: Département de Géologie, Université Laval, Ste-Foy, Québec G1K 7P4.

Acknowledgments

This study was carried out as part of the Canadian Joint Global Flux Study and was supported by the Natural Sciences and Engineering Research Council of Canada. We thank Carlos Vale for providing the samples from the Portuguese continental margin, and George W. Luther for inviting us to participate on a cruise on the RV *Cape Henelopen* in the Chesapeake Bay (supported by NSF grant OCE 93-14349 to G.W. Luther). We thank the captains and the crews of CSS *Alfred Needler*, CSS *Parizeau*, CSS *Hudson*, and RV *Cape Henelopen* for their help at sea.

Table 1. Sampling locations.

Sta.	Depth (m)	Location
Gulf of St Lawrence		
1	360	49°30'N, 66°00'W
2	245	49°40'N, 62°00'W
3	531	47°50'N, 60°05'W
Eastern Canadian shelf and slope		
4	230	43°50'N, 62°49'W
5	830	42°53'N, 61°45'W
Chesapeake Bay		
858-5	16	38°58.84'N, 76°23.15'W
858-6	30	38°58.57'N, 76°22.26'W
858-7	30	38°58.57'N, 76°22.26'W
Portuguese continental margin		
M11	100	38°24.00'N, 09°07.00'W
M36	50	38°24.50'N, 09°07.03'W
S1	2,000	38°10.10'N, 09°35.24'W
T09	1,100	38°10.10'N, 09°35.24'W

the eastern Canadian continental shelf, the Iberian shelf and slope off the coast of Portugal, and the seasonally anoxic part of Chesapeake Bay. The sediments at these sites consisted of clay and silt-size particles. The Canadian sampling sites underlie water with 150–250 μM dissolved oxygen, with the lowest values occurring in the inner part of the Gulf of St. Lawrence. The oxygen penetration depth in the sediments, measured with an oxygen micro-electrode (Silverberg et al. in prep.), varies from 10 to 15 mm, and the oxygen uptake rate by these sediments was estimated at between 2 and 5 mmol cm^{-2} d^{-1}. We do not have corresponding information about the Portuguese sediments, but the bottom water at the sampling sites is well oxygenated (C. Vale pers. comm.). The bottom water at the Chesapeake Bay site was anoxic at the time of sampling.

The cores from the Portuguese shelf and slope and Chesapeake Bay were sampled for solid-phase analysis only. The former were freeze-dried; the latter were squeezed and frozen. The cores from the Gulf of St. Lawrence and the Canadian continental shelf were subsampled into horizontal layers (0.5 cm thick near the surface, 1.0 cm thick deeper in the core) in a glove box under nitrogen (Edenborn et al. 1986). The subsamples were transferred to nylon Reeburgh-type squeezers (Reeburgh 1967) and pore water was extracted at the in situ temperature of 5°C by N_2 pressure applied to a latex membrane. To avoid contact with air, pore waters were filtered in-line through 0.4-μm membrane filters as they exited the squeezers and were collected in 50-cc plastic syringes. The porewater samples were acidified to pH 1.9 (1% equiv vol of trace metal grade HNO_3) and stored at 4°C. The cake of squeezed sediment was placed in plastic bags and kept frozen at −20°C.

The porewater samples were analyzed for dissolved Fe by flame and flameless atomic absorption spectrophotometry (AAS), using the method of standard addition for calibration. Soluble-reactive phosphate was determined colorimetrically as the molybdenum blue complex, using a flow injection system (Ruzika and Hansen 1980). The precision of these analyses was ±5% and the detection limits were 1 μM.

With the exception of the sediments from the Portuguese slope, which had been freeze-dried, the sediment samples were analyzed without drying them first, and the results were corrected for water and salt content. Total Fe and total P were determined by AAS and flow-injection analysis, respectively, of 0.5-g samples that had been digested in a mixture of HF, HCl, HNO_3, and $HClO_4$ according to the procedures described by Sturgeon et al. (1982). The precision of these analyses was ±5% and the accuracy was assured by using the marine sediment reference materials BCSS-1, MESS-1, PACS-1 and BEST-1 (National Research Council of Canada). Pyrite was determined by the sequential extraction method of Lord (1982), and acid-volatile sulfide (AVS = amorphous FeS + mackinawite + poorly crystallized greigite) was determined according the method described by Hsieh and Yang (1989) as modified by Gagnon et al. (1995).

Sediment was subjected to two different partial-extraction techniques to provide information about the forms of Fe and P present. Note that these extractions were not carried out sequentially, for each was performed on a different aliquot of the sample.

Amorphous Fe oxides were determined by ascorbate extraction (Ferdelman 1988; *see* also Kostka and Luther 1994). The ascorbate reagent consists of a deaerated solution of 10 g sodium citrate and 10 g sodium bicarbonate in 200 ml deionized water to which 4 g of ascorbic acid is slowly added for a final pH of 8. About 1 g of wet sediment was extracted with 25 ml of this reagent for 24 h at room temperature (while shaking). The centrifuged and filtered solution was then diluted in 0.1 N HCl and analyzed for Fe and P. Fe was measured by AAS, and P was determined colorimetrically as the molybdenum blue complex by using a flow-injection system. The precision was ±10% for both Fe and P. Total Fe oxides (i.e. amorphous + crystalline oxides) were determined by the citrate-dithionate-bicarbonate (CDB) buffer extraction described by Lucotte and d'Anglejan (1985). The procedure is as follows: 0.25 g sediment was added to 25 ml of a solution containing 0.22 M Na-citrate and 0.11 M $NaHCO_3$ and heated for 15 min at 85–90°C. One-half gram of Na-dithionite was then added (while stirring) at 85–90°C for another 30 min.

The solution was separated from the solid by centrifugation and the sediment was rinsed with 15 ml 1 M NaCl. The centrifuged rinse solution was added to the extractant solution and water was added to make up the volume to 50 ml. This was then divided in two: 25 ml was acidified and analyzed for Fe by AAS. To the other 25 ml we added 0.25 ml of 1 M $FeCl_3$ solution and let it sit 1 week in order to destroy the excess dithionite, which otherwise would interfere with the development of the molybdenum blue complex (Lucotte and d'Anglejan 1985). We then added 4 ml molybdate reagent (0.0405 M ammonium molybdate and 4.0 N sulfuric acid) and 3 ml isobutyl alcohol to a 2-ml sample solution and agitated rapidly for 2 min.

After allowing the phases to separate, the bottom layer was removed and the organic layer was washed with 3 ml of 1 N H_2SO_4. We then added 5 ml of a $SnCl_2$ solution (10.0 g of $SnCl_2$ $6H_2O$ in 25 ml of concentrated HCl, stored <2

d in polyethylene bottle in a refrigerator) and mixed for 1 min. Finally, 1 ml of the colored isobutyl alcohol solution was diluted with 3 ml of 99% ethanol, and the concentration of the molybdate complex was measured at 725 nm after 2 h. Blanks and standards were run through the same procedure. The precision of this analysis is ±5% for Fe and ±7% for P.

Results

Total iron, AVS, and pyrite—These constituents were analyzed in the sediments from the Canadian continental margin. The vertical distribution of total Fe in these sediments ranged from 600 to 1,000 μmol Fe g^{-1} and displayed no clear trend beyond the analytical uncertainty of the measurements (Fig. 1, Table 2). The AVS content was low (<1–7 μmol Fe g^{-1} if all AVS is assumed to be FeS) and showed no discernible trend either regionally or with depth in the cores. Pyrite was present in all the cores. Its concentration was low or undetectable near the sediment surface and increased with depth. The rate of pyrite increase with depth varied regionally. In the Laurentian Trough (Sta. 1 and 3) and Emerald Basin (Sta. 4) sediments the pyrite content increased from undetectable at the surface to 25–100 μmol Fe g^{-1} at 30-cm depth. These observations agree with those reported by Belzile (1988). The pyrite content reached 10–20 μmol Fe g^{-1} at 30-cm depth in the slope (Sta. 5) sediment.

Amorphous and crystalline Fe oxides—Although there were no discernible vertical trends in the total Fe concentrations, the concentrations of both ascorbate-extractable and CDB-extractable iron were clearly highest in the surface layer of the cores from the Canadian and Portuguese continental margins. The distribution of ascorbate-extractable Fe is consistent with the assumption that the ascorbate reagent extracts only the amorphous Fe oxides (Kostka and Luther 1994)—the concentration is highest near the top of the core, decreases rapidly with depth over the top few centimeters, and remains low or undetectable deeper in the cores. The small amount of ascorbate-extractable Fe deeper in the cores could originate from the dissolution of AVS or its oxidation products, both of which are assumed to be soluble in this reagent. Conversely, the distribution of CDB-extractable iron is consistent with the assumption that the CDB reagent extracts both amorphous and crystalline Fe oxides (Lucotte and d'Anglejan 1985; Ruttenberg 1992; Kostka and Luther 1994); that is, against a relatively high and constant background of crystalline iron oxides (on the order of 100 μmol Fe g^{-1}), there is an enrichment of Fe near the sediment surface similar to that measured with the ascorbate extraction. Amorphous Fe oxides are the most reactive of the Fe oxides during early diagenesis (Canfield et al. 1992), and they are likely composed of ferrihydrite, which is the only amorphous Fe oxide known to occur in marine environments. Because the AVS content of these sediments is low in comparison to CDB or ascorbate-extractable Fe, the possible conversion of AVS to Fe oxide during the handling and processing of the samples (Morse 1994) should not affect the results significantly.

The ascorbate reagent extracted similar amounts of Fe from all the Chesapeake Bay sediment samples, but there was no enrichment of ascorbate-extractable Fe in the sediment-surface layer (Table 3). In this highly sulfidic environment it is unlikely to find Fe in the form of amorphous oxides; it is more likely that the ascorbate-extractable Fe is in the form of FeS, which is soluble in the ascorbate reagent. The sulfur content of the sediment at a nearby station has been reported at 0.25–0.40 mmol S g^{-1} DW, which includes pyrite that would not dissolve in the ascorbate reagent (J. Cornwell unpubl. data). The ASC-Fe profiles show low concentrations below the sediment–water interface and may reflect the stepwise conversion of AVS to pyrite.

Total phosphorus—Total P was determined in the sediments from the Canadian continental margin. In these sediments, the total P content decreased rapidly with depth. The difference between the P content at the sediment surface and at 30 cm depth was on the order of 20–30%, in agreement with previous observations from the Laurentian Trough (Sundby et al. 1992). The concentration of total P in the lower parts of the cores varied regionally with the lowest values (15 μmol P g^{-1}) in the continental slope cores and the highest (30 μmol P g^{-1}) in the Laurentian Trough sediment.

CDB and ascorbate-extractable P—Unlike Fe, similar amounts of P were extracted by the two procedures, and there was <3 μmol g^{-1} of extractable P below the P and Fe-enriched surface layer. The distributions of CDB and ascorbate-extractable P are similar and resemble the distribution of ascorbate-extractable Fe. The highest concentrations of extractable P were found near the surface in the cores from both the Canadian and the Portuguese continental margin sediments. The extractable P content in the Chesapeake Bay core was much lower (≤2 μmol g^{-1}) despite the presence of ascorbate-extractable Fe. There was no vertical trend in extractable P in these cores. This also supports the hypothesis that ASC-Fe is not an oxide but most likely FeS.

The Fe : P molar ratio in the ascorbate-extractable fraction was approximately constant within the uppermost first few centimeters of each core (Fig. 2). This is the layer that is enriched in ascorbate-extractable Fe. The Fe : P molar ratios range between 6:1 and 9:1 at the Canadian sites (except Sta. 1), and between 11 : 1 and 14 : 1 at Sta. 1 and at the Portuguese slope sites. In the anoxic Chesapeake Bay sediments, where the P content was low and approximately constant, no such relationship was observed.

Porewater P and Fe—The soluble-reactive phosphate concentration was generally low (5–16 μM) near the sediment–water interface. These concentrations concur with the concentration at which the sediment displays maximum buffer capacity for phosphate (Sundby et al. 1992). They are higher than the phosphate concentration in the bottom water (Yeats 1988), and thus support a net flux of phosphate out of the sediment. At the base of the layer rich in ascorbate-extractable Fe, the concentration of SRP increased with depth. Dissolved Fe, measured on the sediments from the Canadian continental margin, was close to the detection limit

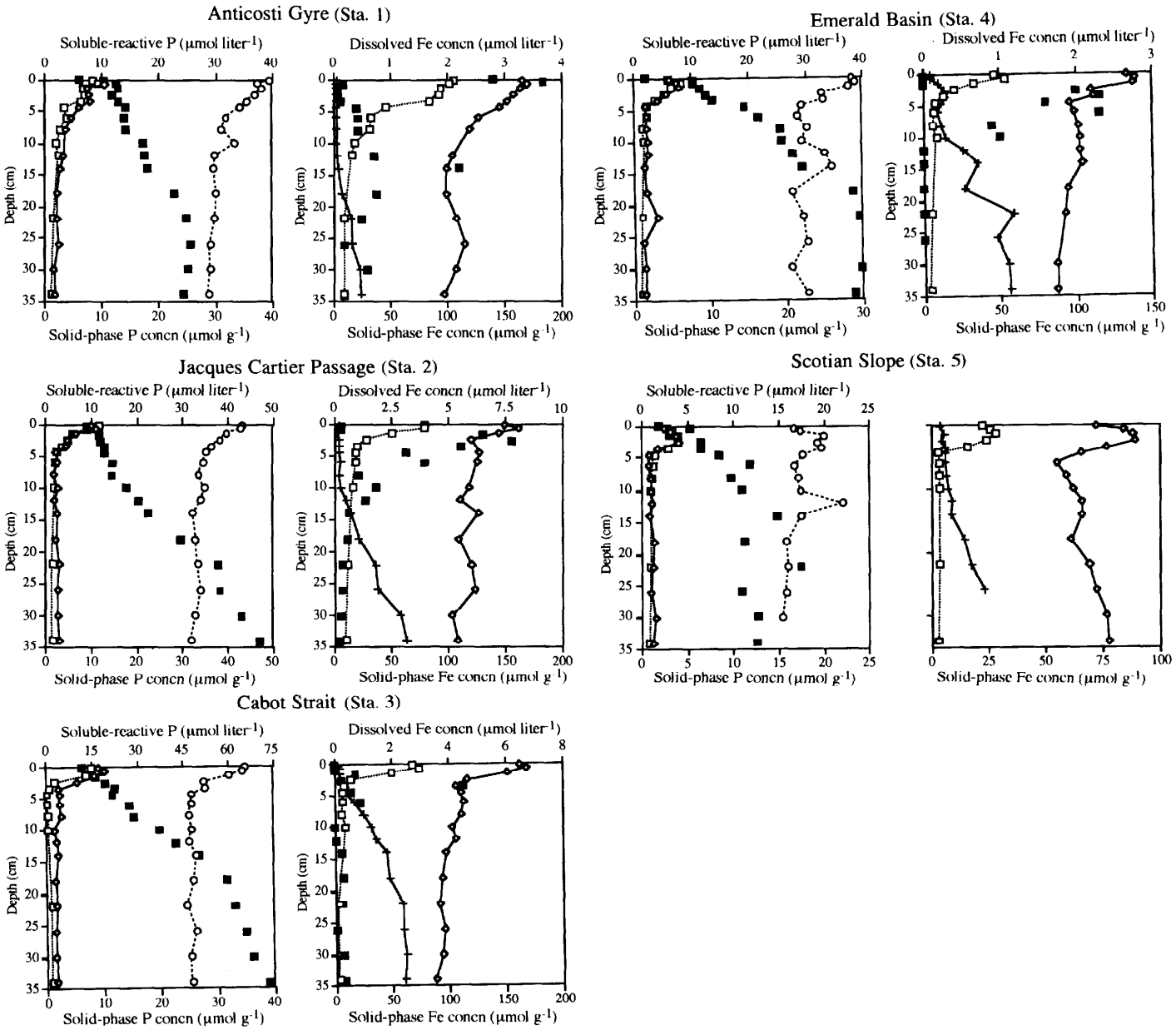

Fig. 1. Vertical profiles of dissolved and extractable phosphorus (left) and iron (right) in sediment cores from five stations located on the Atlantic Canadian continental margin. The concentration units are μmol liter^{-1} (dissolved in the pore water) and μmol g^{-1} (extracted from the solid-phase sediment corrected for sea salt). The sediments were collected in December 1993, except for the Scotian Slope station (May 1993). Total Fe ranged from 600 to 1,000 μmol g^{-1} and is not shown. ■, soluble-reactive P or dissolved Fe; ◇, CDB-extractable P or Fe; □, ascorbate-extractable P or Fe; ○, total P; +, pyrite-Fe.

in the sediment-surface layer. The highest concentrations of dissolved Fe were found near the base of the ascorbate-extractable Fe layer. Deeper in the cores, dissolved Fe decreased to near or below the detection limit.

Discussion

Our data support the notion that only a portion of the P that arrives at the sediment–water interface actually gets trapped within the sediment (Krom and Berner 1981; Balzer 1982; Sundby et al. 1992). Assuming that steady-state conditions prevailed during the sample interval (~30 cm), and considering the decrease in total P content with depth in the cores, our data show that 20–30% of the total P contained in the surface sediment has been remobilized during burial and exported to the overlying water. This estimate is likely to be low, considering that the surface sediment is composed of a mixture of newly deposited material (rich in P) and older P-poor sediment brought to the surface layer by bioturbation. The P that survives burial is not in a form that

Table 2. Ascorbate-extractable iron (ASC-Fe) and phosphorus (ASC-P) in sediments from the Portuguese continental margin and the Chesapeake Bay.

Portuguese continental margin sediments				Chesapeake Bay sediments			
Sta.	Depth (cm)	ASC-P (μmol g^{-1})	ASC-Fe	Sta.	Depth (cm)	ASC-P (μmol g^{-1})	ASC-Fe
M11	0–2	1.92	18.88	858-5	0–1	3.54	51.24
	2–5	1.55	19.64		1–2	1.95	61.74
	5–7.5	1.68	14.82		2–3	1.44	45.59
	7.5–10	1.56	11.65		3–4	1.53	49.51
	12.5–15	1.35	6.85		4–5	1.69	44.83
	20–23	0.72	4.58		5–6	1.28	47.00
					6–7	1.13	52.50
M36	0–2	3.07	37.20		7–8	0.96	47.15
	2–5	2.69	33.85		8–9.3	0.78	25.30
	5–7.5	2.26	26.90		9.3–10	0.90	38.34
	7.5–10	1.95	23.31		10–12.5	0.90	35.91
	10–12.5	1.84	16.72		12.5–14	1.21	31.29
	12.5–15	2.20	9.83				
	15–20	1.26	7.66	858-6	0–0.25	1.56	61.94
	20–25	0.96	8.14		0.25–1.5	1.57	103.38
					1.5–2	1.76	116.31
S1	0–2	7.90	107.51		2–2.5	1.96	109.97
	2–3	5.94	59.82		3–4	2.27	78.64
	3–4	6.74	80.11		4–5	0.92	66.92
	4–5	6.82	94.78		5–6	2.05	65.22
	5–6	4.01	25.93		7–8	1.00	85.91
	6.5–7	4.35	26.02		10–11	1.84	86.48
	7–8	3.50	26.28		13–15	1.01	76.99
	8–9	3.55	22.46		24–26	1.91	51.07
	9–10	3.75	26.04		34–36	2.11	34.32
	11–12	2.89	20.53				
	13–14	4.70	44.50	858-7	0–0.5	1.51	76.52
					0.5–1	1.41	106.50
T09	0–1	5.47	74.35		1–1.5	1.04	99.92
	1–2	5.54	71.22		1.5–2	1.15	73.48
	2–3	4.71	60.93		2–2.5	0.37	66.87
	3–4	4.68	56.69		2.5–3	0.62	72.44
	4–5	4.63	48.29		3–3.5	0.90	60.63
	6–7	4.22	38.73		4–5	1.17	60.84
	8–9	3.94	23.00		6–8	0.83	76.38
	10–11	3.41	20.47		10–12	0.43	59.68
	12–13	3.47	19.69		14–16	0.50	34.04
	14–15	3.45	16.77				
	29–31	2.88	13.35				

can be extracted by either ascorbate or CDB, and the concentration of this P is nearly constant with depth. Because the CDB reagent is known as an efficient extractant of sedimentary Fe oxide phases and the P adsorbed on and coprecipitated with these phases, the P that is buried and preserved must be associated with other sediment components. A possible candidate is apatite (igneous apatite and fish debris), the main P-bearing mineral in the sediments of the St. Lawrence Estuary (Lucotte and d'Anglejan 1985).

An estimate of the importance of the phosphate flux from the Canadian continental margin sediments can be made by using the porewater data and diffusion calculations and by using the labile solid-phase P distribution and estimates of sediment accumulation rates. Both approaches require certain assumptions. The diffusive flux of phosphate across the sediment–water interface (J) can be calculated via Fick's first law of diffusion:

$$J = D\ (\mathrm{d}C/\mathrm{d}z),$$

where D is the diffusion coefficient of PO_4 in porewater (115 cm^2 yr^{-1}; Krom and Berner 1981) and $\mathrm{d}C/\mathrm{d}z$ is the concentration gradient at the sediment–water interface. The measured concentration difference between the top 0.5 cm of sediment and the bottom water at several stations ranges from 1.8 to 8.9 nmol cm^{-3}. If we assign the porewater concentration to the center of the sampled depth interval (i.e. 0.25 cm), the bottom-water value to the sediment surface, and assume a linear gradient between the surface and 0.25 cm, the phosphate gradients range from 7.2 to 35.6 nmol cm^{-4} and we obtain diffusive fluxes of 0.83–4.1 μmol cm^{-2}

Table 3. Composition of pore water and sediments at five stations located on the Atlantic Canadian continental margin (Fe_{tot}, total iron; P_{tot}, total phosphorus; AVS, acid-volatile sulfur; FeS_2, pyrite; CDB-Fe and CDB-P, iron and phosphorus extracted with a citrate-dithionite-bicarbonate buffer; ASC-Fe and ASC-P, iron and phosphorus extracted with ascorbate. The solid-phase analyses have been corrected for the presence of sea salts).

		Solid-phase Fe					Solid-phase P			Pore water	
Sta.	Depth (cm)	Fe_{tot}	AVS	FeS_2	CDB-Fe	ASC-Fe	P_{tot}	CDB-P	ASC-P	PO_4	Fe
		(μmol g^{-1})								(μmol liter $^{-1}$)	
1, Dec	0									6.1	2.8
	0–0.5	1,022	0.18	1.8	164.6	105.0	39.5	10.2	8.3	10.3	3.6
	0.5–1	914	0.29	1.9	168.5	101.8	37.3	10.3	9.4	12.4	0.2
	1–2	909	0.26	1.8	162.7	93.6	37.9	7.4	6.8	12.8	0.1
	2–3	944	0.30	1.7	157.2	91.8	37.0	7.6	7.0	11.7	0.1
	3–4	906	0.33	1.6	152.2	83.6	35.4	7.8	6.1	12.8	0.1
	4–5	914	0.34	1.7	144.8	46.0	34.2	6.0	3.3	14.1	0.4
	5–6	901	0.43	1.8	126.9	32.3	31.7	4.6	3.8	13.7	0.4
	6–7	845	0.47	1.9	119.1	32.0	31.0	3.5	2.8	14.1	0.4
	7–9	862	0.48	1.7		18.5	33.4		2.0	17.3	0.4
	9–11	845	0.50	2.6	103.8	15.4	29.8	3.2	2.3	17.4	0.7
	11–13	869	0.53	3.8	99.0		29.6	2.6		17.8	2.2
	15–17	858	0.51	6.6	98.3		29.9	2.1		22.7	0.8
	19–21	868	0.41	15.0	108.2	8.8	29.7	2.1	1.6	24.8	0.5
	23–25	839	0.63	15.9	114.9		29.0	2.4		25.6	0.2
	27–29	883	0.61	22.9	106.4		29.0	1.5		24.9	0.6
	31–33	860	0.43	23.9	96.5	9.1	28.8	1.8	1.2	24.4	0.2
2, Dec	0									2.0	
	0–0.5	908	0.36	3.4	148.4	78.5	43.4	10.0	11.9	9.0	0.3
	0.5–1	863	0.38	3.2	160.5	78.5	42.7	11.0	10.3	9.0	0.2
	1–2	810	0.55	3.1	144.1	51.2	39.9	6.9	6.0	11.6	6.5
	2–3	808	0.52	3.3	119.4	27.9	38.2	4.7	4.7	12.0	7.7
	3–4	818	0.47	3.3		19.3	36.3	4.6	3.7	12.7	5.5
	4–5	819	0.50	3.6	127.1	18.6	35.3	2.4	2.5	12.9	3.1
	5–7	816	0.45	4.3	125.0	18.3	34.5	2.5	2.4	14.7	3.9
	7–9	823	0.62	3.8			33.6	1.9		14.6	1.0
	9–11	835	0.65	5.1	118.2	15.8	34.8	2.7	2.1	17.6	1.8
	11–13	831	0.84	10.1	110.1		34.0	2.1		20.2	1.3
	13–15	817	1.35	13.3	125.8		32.3	2.5		22.5	0.6
	17–19	829	1.00	20.4	108.6		32.9	2.4		29.4	0.5
	21–23	827	1.36	35.8	120.2	12.0	33.2	2.9	1.5	37.7	0.3
	25–27	859	2.17	38.1	122.7		34.2	2.8		38.2	0.4
	29–31	858	1.72	58.1	103.1		32.8	2.8		42.9	0.3
	33–35	860	1.32	63.2	107.8	9.9	31.8	3.0	1.6	47.0	0.2
3, Dec	0									2.0	1.0
	0–0.5	752	0.25	2.9	161.6	68.0	35.1	9.3	8.0	11.4	0.0
	0.5–1	750	0.16	3.4	167.7	74.0	34.6	10.3	9.2	14.5	0.0
	1–2	732	0.15	3.7	150.6	50.0	32.3	8.5	7.0	16.0	0.7
	2–3	702	0.36	5.2	116.0	14.0	27.6	5.4	1.6	19.4	0.2
	3–4	720	0.37	8.3	105.6	7.5	27.9	2.2	0.7	22.5	4.5
	4–5	709	0.36	8.7	111.1	6.6	25.6	2.4	0.3	21.5	0.6
	5–7	717	0.47	16.4	113.1	6.8	25.4	2.5	0.3	27.3	0.9
	7–9	720	0.52	24.5	110.7	6.2	25.0	2.6	0.5	28.6	0.2
	9–11	733	0.50	31.3	102.6	8.3	25.7	1.4		37.1	0.0
	11–13	752	0.75	35.4	105.5		25.0	1.8		42.2	0.0
	13–15	761	0.55	44.8	97.1		26.3	2.0		49.8	0.2
	17–19	749	0.74	47.9	93.6		25.9	1.6		59.0	0.3
	21–23	779	1.07	59.1	91.9	2.6	24.6	1.8	1.0	62.0	0.2
	25–27	692	0.67	59.3	95.4		26.3	1.7		65.5	0.0
	29–31	744	0.44	61.6	94.0		25.2	1.6		67.7	0.3
	33–35	722	0.44	60.3	87.3	2.8	25.5	1.8	0.7	73.1	0.3

Table 3. Continued.

Sta.	Depth (cm)	Solid-phase Fe					Solid-phase P			Pore water	
		Fe_{tot}	AVS	FeS_2	CDB-Fe	ASC-Fe	P_{tot}	CDB-P	ASC-P	PO_4	Fe
		(μmol g^{-1})								(μmol liter $^{-1}$)	
4, Dec	0									2.0	
	0–0.5	742		4.5	133.6	46.9	28.8	4.7	4.6	10.1	0.0
	0.5–1	719	0.33	4.5	138.9	54.1	29.1	5.6	6.2	10.3	0.0
	1–2	724	0.20	9.8	137.3	33.3	28.2	5.9	4.8	11.4	0.0
	2–3	692	0.14	13.0	110.3	20.0	24.7	4.2	4.1	12.4	2.0
	3–4	673	0.24	14.2	111.8	12.5	24.8	3.0	2.7	13.6	2.3
	4–5	751	0.34	10.9	95.9	7.1	22.2	1.6	1.8	19.1	1.6
	5–7	697	0.39	9.0	98.6	6.3	21.5	1.7	1.7	21.7	2.3
	7–9	723	0.36	11.3	101.6	5.7	22.8	1.7	1.1	25.6	0.9
	9–11	741	0.31	14.1	102.2	8.2	22.1	1.9	1.3	25.8	1.0
	11–13	690	0.32	26.3	102.7		25.1	1.9		27.5	0.0
	13–15	728	0.61	34.9	103.8		26.1	1.5		29.1	0.0
	17–19	688	0.30	26.8	94.1		20.7	1.7		38.3	0.0
	21–23	717	0.32	58.8	93.1	5.1	22.3	3.0	1.0	39.4	0.0
	25–27	751	0.33	47.5			22.8	1.3		41.1	0.0
	29–31	753	0.42	55.5	87.1		20.6	1.4		39.7	
	33–35	747	0.31	56.3	86.9	3.4	22.7	1.5	0.9	38.6	
4, May	0									1.3	
	0–0.5	795	0.00	11.2	137.7	61.7	30.0	6.3	7.7	7.5	
	0.5–1	807	0.00	11.6	141.1	63.0	27.8	7.1	7.6	7.5	
	1–2	789	2.91	15.1	126.5	39.0	26.4	5.4	5.0	5.7	
	2–3	779	1.12	17.0	108.3	23.9	26.0	3.9	4.1	7.5	
	3–4	753	0.55	22.7	109.9	10.8	21.8	2.8	2.4	7.9	
	4–5	750	0.61	28.8	134.4	10.8	21.2	3.6	2.0	8.7	
	5–7	749	0.87	42.9	101.9	9.5	21.6	2.1	1.9	11.1	
	7–9	754	1.31	74.9	103.6	10.8	20.6	2.0	2.1	10.9	
	9–11	775	0.79	95.2	102.9	10.2	20.4	1.9	2.0	10.9	
	11–13	762	1.13	103	99.6		19.8	2.0		10.6	
	13–15	769	1.24	100	92.0		19.9	1.6		12.1	
	17–19	734	0.99	116	87.0	6.3	19.8	2.0	1.8	11.2	
	21–23	801	1.52	114	84.8		20.5	1.7		10.9	
	25–27	801	1.59	116	85.7		19.3	1.8		14.8	
	29–31	803	1.50	107	81.2		19.8	1.8		10.1	
	33–35	772	1.21	108	80.2	4.7	19.2	2.1	1.5	12.9	
5, May	0									1.9	
	0–0.5	483	0.63	3.6	71.8	22.8	16.6	2.4	2.7	5.2	
	0.5–1	510	0.26		84.0	26.0	17.3	3.1	3.4		
	1–2	522	0.32	5.6	87.9	28.6	20.0	3.7	3.9	3.0	
	2–3	538	0.24	4.8	89.1	24.1	19.2	4.0	3.8	6.5	
	3–4	546	0.46	5.9	76.8	16.2	19.6	1.7	2.9	6.5	
	4–5	516	0.35	5.9	65.4	3.1	17.5	0.7	1.3	8.4	
	5–7	506	0.32	6.1	55.0	3.5	16.7	0.7	1.2	11.7	
	7–9	517	0.35	6.6	59.1	3.6	17.1	1.0	1.1	9.8	
	9–11	516	0.60	6.9	62.2	3.3	17.4	1.0	1.0	10.9	
	11–13	533	0.59	8.9	66.3		22.0	1.0			
	13–15	547	0.42	8.7	66.0		17.4	0.9		14.7	
	17–19	547	0.47	14.6	61.2		15.8	1.3		11.2	
	21–23	610	0.73	17.6	69.2	3.7	15.9	1.2	1.0	17.4	
	25–27	594	0.45	23.1	72.2		15.7	0.9		10.9	
	29–31	626	0.35		76.4		15.4	1.5		12.8	
	33–35		0.62		77.8	3.3		1.2	0.8	12.5	

yr^{-1}. In order to use the solid-phase data, we must assume values for the sediment accumulation rate (attempts to measure it by using ^{210}Pb were confounded by the problem of accounting for the effect of bioturbation on the ^{210}Pb activity profile). Our best estimate of the sediment accumulation used 1 mm yr^{-1} or 75 mg cm^{-2} yr^{-1}, estimated for sites in the Laurentian Through near Sta. 1 and 3 (Silverberg et al. 1986). Multiplying the loss of P with depth (10 μmol g^{-1}) by this sedimentation rate gave a flux of 0.75 μmol cm^{-2} yr^{-1} phosphate from the sediment. This value is at the low

Table 3. Continued.

Sta.	Depth (cm)	Solid-phase Fe					Solid-phase P			Pore water	
		Fe_{tot}	AVS	FeS_2	CDB-Fe	ASC-Fe	P_{tot}	CDB-P	ASC-P	PO_4	Fe
		(μmol g^{-1})								(μmol $liter^{-1}$)	
1, June	0									6.4	1.7
	0–0.5	899	1.52	0.9		127.6	39.3		9.9	8.2	1.0
	0.5–1	981	0.48	1.1		128.4	40.2		10.0	8.2	0.8
	1–2	948	0.54	1.0		124.0	38.5		9.5	9.0	1.0
	2–3	968	0.64	1.1		122.0	37.1		8.9	10.9	0.7
	3–4	978	0.65	1.7		110.6	35.9		7.9	13.3	0.9
	4–5	981	0.62	1.3		109.9	35.0		9.1	14.2	0.8
	5–6	875	0.54	1.4		51.8	30.4		4.8	12.6	0.8
	6–7	926	0.83	1.7		21.4	29.9		2.2	12.4	1.8
	7–9	927	0.99	1.9		13.4	30.9		2.0	15.4	1.2
	9–11	882	1.45	3.7			29.1			19.4	1.1
	11–13	899	1.81	9.7			29.4			18.7	1.8
	15–17	899	1.56	15.7			27.2			25.3	0.7
	19–21	902	3.52	20.0		11.6	27.4		1.8	33.3	2.7
	23–25	927	2.58	24.3			27.9			37.7	2.6
	27–29	924	1.57	24.0			27.5			35.7	9.3
	31–33	899	3.05	24.4		12.1	27.5		0.9	40.6	1.2
2, June	0									4.0	0.5
	0–0.5	844	1.54	5.6		46.6	38.3		8.0	12.9	0.7
	0.5–1	846	2.30	6.4		37.0	37.3		6.4	12.7	0.5
	1–2	857	1.49	9.2		28.2	34.2		4.4	10.8	3.3
	2–3	858	2.91	17.8		22.5	35.3		3.1	9.3	6.5
	3–4	844	4.03	13.9		18.2	34.2		1.7	11.9	16.2
	4–5	841	3.15	25.4		18.4	31.5		1.6	11.1	10.9
	5–7	849	3.98	31.9		19.3	29.8		1.6	11.2	4.6
	7–9	840	4.70	33.4		18.3	33.4		1.6	12.5	5.1
	9–11	843	4.63	36.5		18.0	30.0		1.0	12.5	1.1
	11–13	850	5.70	53.1			29.5			15.4	1.8
	13–15	859	6.62	45.3			31.8			15.5	0.9
	17–19	849	2.91	44.5			30.4			20.4	0.6
	21–23	841	1.94	50.6		7.0	30.7		0.8	21.1	1.7
	25–27	836	3.06	60.9			32.4			26.8	1.9
	29–31	862	2.50	63.9			32.5			26.4	0.4
	33–35	873	3.23	71.2		6.6	31.8		0.9	28.5	0.5
3, June	0									2.4	0.9
	0–0.5	837	1.14	2.9		73.3	35.0		10.7	8.1	0.5
	0.5–1	812	2.53	2.5		38.3	29.7		6.6	11.0	0.5
	1–2	781	1.98	2.3		13.6	26.0		3.0	13.4	0.7
	2–3	807	4.03	2.5		11.8	25.7		2.0	16.2	3.9
	3–4	811	3.86	2.6		11.8	26.3		1.4	16.6	0.6
	4–5	789	4.06	3.0		13.2	25.7		1.8	19.7	0.5
	5–7	787	2.96	4.1		9.6	24.6		1.0	33.7	1.1
	7–9	793	3.48	6.6		8.1	25.7		1.5	38.1	0.6
	9–11	781	3.50	9.6		7.8	25.4		1.2	41.8	0.8
	11–13	795	2.13	15.2			25.4			40.7	0.6
	13–15	783	3.08	21.3			25.5			46.5	0.5
	17–19		3.52	28.7			25.3			51.4	2.2
	21–23	800	2.37	36.8		5.0	24.4		1.5	58.5	1.1
	25–27	803	4.71	44.4			26.1			61.6	0.6
	29–31	792	4.70	43.1			25.8			57.4	0.6
	33–35		6.67	49.2		4.9			1.3	60.0	1.1

end of the range obtained via the diffusion calculation, and because it is probably an underestimate, we conclude that the flux of phosphate from these sediments could be in the range of 1–4 μmol cm^{-2} yr^{-1}.

The reason why P is released to the overlying water is that the sediment loses its capacity to adsorb phosphate as it undergoes burial. The loss of adsorption capacity has been attributed to the progressive reductive dissolution of amorphous Fe in the anoxic subsurface-sediment layers (Krom and Berner 1980; Sundby et al. 1992; Jensen et al. 1995).

Table 3. Continued.

Sta.	Depth (cm)	Solid-phase Fe					Solid-phase P			Pore water	
		Fe_{tot}	AVS	FeS_2	CDB-Fe	ASC-Fe	P_{tot}	CDB-P	ASC-P	PO_4	Fe
		(μmol g^{-1})								(μmol $liter^{-1}$)	
4, June	0									2.1	0.4
	0–0.5	778	1.42	2.9		63.7	27.3		7.3	5.2	0.6
	0.5–1	746	1.35	3.2		41.3	24.4		5.5	5.2	5.5
	1–2	750	1.60	4.2		13.3	21.7		2.5	6.3	0.8
	2–3	779	1.59	6.0		7.7	21.5		1.4	9.5	10.0
	3–4	724	1.60	11.2		8.2	17.8		1.2	10.2	3.1
	4–5	744	1.55	11.5		7.3	19.8		1.0	9.9	2.5
	5–7	739	1.64	13.1		7.8	18.3		0.9	10.7	4.3
	7–9	598	1.90	13.3		7.4	17.6		1.3	10.2	3.9
	9–11	737	1.51	16.1		7.2	19.0		0.4	10.2	2.2
	11–13	669	1.63	23.9			18.3			11.7	1.8
	13–15	739	1.69	20.1			20.1			11.5	1.0
	17–19	793	1.57	24.2			19.8			20.4	10.0
	21–23	751	1.26	33.0		3.7	19.4		0.7	25.1	0.9
	25–27	742	1.52	44.3			21.4			18.8	1.8
	29–31	734	1.55	53.4			19.8			21.4	0.3
	33–35	745	1.55	53.7		3.1	20.3		0.9	26.9	0.4
5, June	0									2.0	
	0–0.5	492	0.60	1.8		29.6	19.1		3.7	6.9	0.7
	0.5–1	508	0.45	1.4		27.3	20.0		3.0	9.3	1.8
	1–2	530	0.63	1.7		19.9	18.5		1.9	6.9	0.9
	2–3	548	0.56	1.2		18.4	17.8		2.1	6.9	0.7
	3–4	539	0.72	1.0		17.7	18.0		1.8	7.7	0.5
	4–5	573	0.44	1.3		7.8	16.7		1.3	9.3	0.6
	5–7	505	0.52	1.4		2.7	16.9		0.7	10.1	0.8
	7–9	524	0.39	1.6		4.1	14.4		0.8	15.4	0.9
	9–11	507	0.66	2.0		3.5	17.9		0.8	17.0	8.6
	11–13	563	0.50	1.9			17.9			23.5	1.6
	13–15	524	0.52	2.6			16.7			23.1	1.3
	17–19	516	0.72	4.9			17.1			15.8	0.9
	21–23	540	0.68	4.2		2.2	16.4		0.7	18.7	1.5
	25–27	549	0.83	6.4			14.9			14.2	2.6
	29–31	548	0.92	9.7			16.1			17.8	2.6
	33–35	530	0.65	12.5		2.2	16.1		0.9	12.2	3.8

In agreement with this, we observed that the contents of amorphous Fe oxides and extractable P (CDB or ascorbate) in the sediments from the Canadian and Portuguese continental margin sites decrease simultaneously with depth in the sediment. Several mechanisms may explain this phenomenon: (1) amorphous Fe oxides may react directly with HS^- to form FeS, (2) they may be converted to more crystalline oxides, (3) they may be reprecipitated as a nonextractable (by CDB) mineral species, and (4) they may be used as terminal electron acceptors in the bacterial oxidation of organic carbon.

The first of these possibilities, the direct formation of FeS, may well be the controlling mechanism in the highly sulfidic Chesapeake Bay sediments. In the Canadian and Portuguese margin sediments, the AVS concentration is low, but this could be due to a rapid conversion of FeS to pyrite. The second possibility, the conversion to more crystalline iron oxides, seems unlikely because the high P:Fe ratio in the ascorbate extract indicates that most of the surface sites of the Fe phase are occupied by phosphate ions. The abundance of phosphate ions on the surface may block the sites needed for crystal growth and prevent recrystallization. The inhibition of ferrihydrite recrystallization by saturation of its surface sites by SiO_4^{4-} has been reported in previous studies (Carlson and Schwertmann 1981; Karim 1984; Zhao et al. 1994). Although ferrihydrite is known to convert slowly to hematite or goethite (Schwertmann and Murad 1983; Fisher and Schwertmann 1975; Cornell 1988), the absence of an increase in CDB-extractable Fe to compensate for the disappearance of amorphous Fe undermines the recrystallization mechanism as an explanation for the disappearance of amorphous Fe oxides during burial. If recrystallization to a more crystalline Fe oxide occurred, it is likely that only part of the phosphate would be readsorbed, although to a smaller extent because of the loss in reactive surface area. The third possibility, the precipitation of an authigenic Fe(II) mineral other than sulfide (e.g. siderite, mixed Fe-Ca carbonates, or an Fe-rich silicate) can be neither discounted nor confirmed. Nor can we eliminate the use of Fe oxides as terminal electron acceptors since we observed an Fe peak in the distribution of dissolved Fe at the depth where ascorbate-extractable Fe disappears.

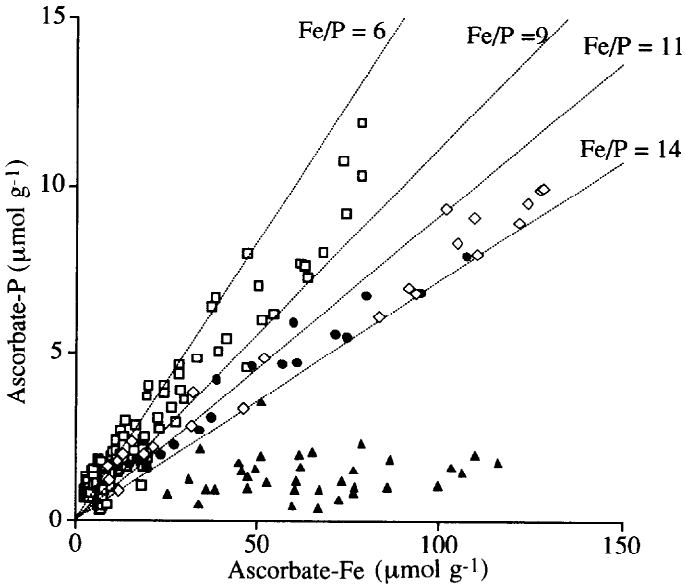

Fig. 2. Plot of ascorbate-extractable Fe vs. ascorbate-extractable P for the sediments from the Eastern Canadian continental margin, the Portuguese continental slope, and the Chesapeake Bay. The plot shows nearly linear relationships with values of the Fe:P ratio between 6 and 9 for Sta. 2, 3, 4, and 5 (□) and between 11 and 14 for Sta. 1 (◇) and the Portuguese continental slope (●). No relationship could be discerned for the sediments from Chesapeake Bay (▲).

Because of the low adsorption capacity of pyrite for phosphate (Krom and Berner 1980), the conversion of amorphous Fe oxides to pyrite would release phosphate to the pore waters and create a concentration gradient driving a flux of phosphate toward the sediment surface. The FeS_2 content does indeed increase as ascorbate Fe disappears. Assuming that Fe does not escape from the sediment to the water column, we expect to find approximately as much pyrite Fe at depth in the sediment as amorphous Fe oxide in the surface sediment. With the exception of the two cores from Sta. 1, where we think that pyritization is continuing beyond our sampling depth, the concentration of pyrite iron at 30-cm depth is indeed similar to the amorphous Fe concentration in the surface sediment.

The proposed conversion of amorphous Fe oxides to pyrite requires the reductive dissolution of Fe oxides at the base of the enriched surface layer and downward transport of reduced Fe. At steady state, and assuming no loss of dissolved Fe to the water column from the oxic surface sediment, the concentration of solid-phase Fe should then display a minimum at the depth where the reductive dissolution takes place. We in fact observed a minimum in the sum of pyrite plus ascorbate extractable iron (ΣFe-Py + Fe-ASC) in all our cores. There is also a minimum in the sum of pyrite plus CDB-extractable iron (ΣFe-Py + Fe-CDB). The mechanism of downward transport is more problematic, however. Because the pyrite content increases gradually to the bottom of the cores and because AVS, which is the precursor of pyrite (Schoonen and Barnes 1991; Gagnon et al. 1995) was present (albeit in low concentrations) at all depths below the surface layer, it seems that pyritization occurs over a large depth interval from below the amorphous oxide-containing surface layer to the bottom of the core. This requires the availability of pyritizable Fe throughout the core. Because dissolved Fe quickly becomes undetectable below the depth where amorphous Fe disappears, it does not seem that the Fe for pyrite formation was supplied by diffusion in the pore water. Nor would it appear that it was transported as AVS-Fe because of the low concentrations of AVS-Fe throughout the cores. Given these observations, if we assume steady state, we conclude that the Fe used in pyrite formation is supplied via the burial of unknown but more refractory solid phases that incorporate Fe at the bottom of the amorphous Fe oxide-rich layer. As this phase undergoes burial, the Fe it contains reacts with HS^- to form first FeS and then pyrite without releasing Fe(II) to the pore waters. Canfield et al. (1992) estimated the reactivity (half-life) of various Fe minerals with respect to sulfidization and proposed that this reaction proceeds with depth, although slowly, as these phases are reduced and the Fe(II) is incorporated with pyrite. A comparison of CDB and 1 N HCl-extractable Fe from sediments taken in the estuary revealed that Fe is probably released from silicates by the HCl treatment and is available to sulfidization (A. Bono pers. comm.)

The nature of the associations of P with Fe is indicated by the Fe:P molar ratio in the sediment, particularly in the sediment surface layer that contains the reactive (mobile) P fraction. Previous estimations of the Fe:P ratio in the sediment fraction extracted by CDB have suggested that a ratio in the range of 20–26 is characteristic of modern oxic sediments in the North Atlantic and the Labrador Sea (De Lange 1986; Lucotte et al. 1994). We found similar values in the CDB extract of the surface sediment in our cores (Fe:P = 14–29). However, because CDB extracts not only the amorphous Fe oxide fraction, to which all the mobile P is adsorbed, but also the more crystalline Fe oxides, it is perhaps more appropriate to consider the Fe:P ratio in the ascorbate-extractable fraction. Accordingly, we found that the ratio was smaller and less variable (Fig. 2). Furthermore, we found that the relationship between ascorbate-extractable P and Fe was linear within each core. At four of the five eastern Canadian sites, the molar relationship between ascorbate-extractable P and Fe was described by $P = 0.13 \times Fe + 0.15$ ($r^2 = 0.897$) and an average Fe:P ratio of 7.7. For the surface sediment from Sta. 1 and the Portuguese slope sites, the molar relationship is $P = 0.073 \times Fe + 0.5$ ($r^2 = 0.94$), with an average Fe:P ratio of 13.7. There is no such relationship for the anoxic sediments from Chesapeake Bay, because the sediment surface is anoxic and does not contain amorphous Fe oxides.

The low and relatively invariant Fe:P ratios suggest the existence of an Fe oxide phase with very high adsorption capacity (i.e. a very large specific surface area). Canfield et al. (1992) and Raiswell (1993) have shown that ferrihydrite is the most reactive Fe oxide phase present in marine sediment. Crystallographic studies have revealed that 30-Å-diameter spherical ferrihydrite particles (which are typical of these natural authigenic phases; Waychunas et al. 1994; Zhao et al. 1994) may expose as much as 30% of their Fe content as coordination-unsaturated ferric ions at the surface (Waychunas et al. 1994; Zhao et al. 1994). Because HPO_4^{2-},

the dominant soluble-reactive P species in seawater, can occupy two coordination sites (Sigg and Stumm 1981), the Fe:P ratio of a 30-Å phosphate-saturated spherical ferrihydrite phase can reach 6.7. This is close to the value of 7.7 that we observed in the ascorbate-extractable fraction of eastern Canadian surface sediments. This suggests that the phosphate-bearing phase extracted with ascorbate is most likely ferrihydrite, with most of the sorption sites occupied by phosphate. More Fe oxide, as in the sediments from the Portuguese margin and Sta. 1, would imply larger authigenic particles or thicker coatings on other particles and therefore fewer surface adsorption sites per unit weight or volume. In turn, this would lead to higher Fe : P ratios, as observed.

Because of the strong affinity of Fe oxides for phosphate, the Fe oxide-rich sediment layer has been described as a trap for phosphate (Mortimer 1971). In sediments such as those studied here, where 20–30% less P is buried than arrives at the sediment–water interface, the surface layer should not be thought of as a trap, for some of the phosphate released deeper in the sediment can escape successfully to the water column. It is better to think of the iron-rich surface layer as a regulator of the phosphate flux out of the sediment: The porewater concentration of phosphate is buffered by sorption equilibria with the sediment at a value higher than in the overlying water. This gives rise to a concentration gradient across the sediment–water interface that supports a phosphate flux out of the sediment, and in order to replace the dissolved phosphate that escapes, the sediment releases phosphate to the pore water (Sundby et al. 1992).

References

BALZER, W. 1982. On the distribution of iron and manganese at the sediment/water interface: Thermodynamic versus kinetic control. Geochim. Cosmochim. Acta **48:** 1153–1161.

———. 1986. Forms of phosphorus and its accumulation in coastal sediments of Kieler Bucht. Ophelia **26:** 19–35.

BELZILE, N. 1988. The fate of arsenic in sediments of the Laurentian Trough. Geochim. Cosmochim. Acta **52:** 2293–2302.

BROECKER, W. S. 1982. Ocean chemistry during glacial time. Geochim. Cosmochim. Acta **46:** 1689–1705.

CANFIELD, D. E., R. RAISWELL, AND S. BOTTRELL. 1992. The reactivity of sedimentary iron minerals toward sulfide. Am. J. Sci. **292:** 659–683.

CARACO, N., J. COLE, AND G. E. LIKENS. 1990. A comparison of phosphorus immobilization in sediments of freshwater and coastal marine systems. Biogeochemistry **9:** 277–290.

CARLSON, L., AND U. SCHWERTMANN. 1981. Natural ferrihydrites in surface deposits from Finland and their association with silica. Geochim. Cosmochim. Acta **45:** 421–429.

CORNELL, R. M. 1988. The influence of some divalent cations on the transformation of ferrihydrite to more crystalline products. Clays Clay Min. **23:** 329–332.

DE LANGE, G. J. 1986. Early diagenetic reactions in interbedded pelagic and turbiditic sediments in the Nares Abyssal Plain (western North Atlantic): Consequences for the composition of sediment and interstitial water. Geochim. Cosmochim. Acta **50:** 2543–2564.

EDENBORN, H., A. MUCCI, N. BELZILE, J. LEBEL, N. SILVERBERG, AND B. SUNDBY. 1986. A glove-box for the fine-scale subsampling of sediment box-cores. Sedimentology **33:** 147–150.

FERDELMAN, T. G. 1988. The distribution of sulfur, iron, manganese, copper and uranium in salt marsh sediment cores as determined by sequential extraction methods. M.Sc. thesis, University of Delaware.

FISHER, W. R., AND U. SCHWERTMANN. 1975. The formation of hematite from amorphous iron(III) hydroxide. Clays Clay Min. **23:** 33–37.

FROELICH, P. N., M. L. BENDER, N. A. LUEDTKE, G. R. HEATH, AND T. DEVRIES. 1982. The marine phosphorus cycle. Am. J. Sci. **282:** 474–511.

GAGNON, C., A. MUCCI, AND E. PELLETIER. 1995. Anomalous accumulation of acid-volatile sulphides (AVS) in a coastal marine sediment, Saguenay Fjord, Canada. Geochim. Cosmochim. Acta **59:** 2663–2675.

HOWARTH, R. W., H. S. JENSEN, R. MARINO, AND H. POSTMA. 1995. Transport and processing of phosphorus in estuaries and oceans, p. 323–345. *In* Phosphorus cycling in terrestrial and aquatic ecosystems. SCOPE, Wiley.

HSIEH, Y. P., AND C. H. YANG. 1989. Diffusion methods for the determination of reduced inorganic sulfur species in sediments. Limnol. Oceanogr. **34:** 1126–1130.

JENSEN, H. S., P. B. MORTENSEN, F. Ø. ANDERSEN, E. RASMUSSEN, AND A. JENSEN. 1995. Phosphorus cycling in a coastal marine sediment, Aarhus Bay, Denmark. Limnol. Oceanogr. **40:** 908–917.

KARIM, Z. 1984. Characteristics of ferrihydrites formed by oxidation of $FeCl_2$ solutions containing different amounts of silica. Clays Clay Min. **32:** 131–184.

KOSTKA, J. E., AND G. W. LUTHER III. 1994. Partitioning and speciation of solid phase iron in saltmarsh sediments. Geochim. Cosmochim. Acta **58:** 1701–1710.

KROM, M. D., AND R. A. BERNER. 1980. Adsorption of phosphate in anoxic marine sediments. Limnol. Oceanogr. **25:** 797–806.

———, AND ———. 1981. The diagenesis of phosphorus in a nearshore marine sediment. Geochim. Cosmochim. Acta **45:** 207–216.

LORD III, C. J. 1982. A selective and precise method for pyrite determination in sedimentary material. J. Sed. Petrol. **48:** 664–666.

LUCOTTE, M., AND B. D'ANGLEJAN. 1985. A comparison of several methods for the determination of iron hydroxides and associated orthophosphates in estuarine particulate matter. Chem. Geol. **48:** 257–264.

———, A. MUCCI, C. HILLAIRE-MARCEL, AND S. TRAN. 1994. Early diagenetic processes in deep Labrador Sea sediments: Reactive and nonreactive iron and phosphorus. Can. J. Earth Sci. **31:** 14–27.

MORSE, J. W. 1994. Interaction of trace metals with authigenic sulfide minerals: Implication for their bioavailability. Mar. Chem. **46:** 1–6.

MORTIMER, D. H. 1971. Chemical exchanges between sediments and water in the Great Lakes—speculations on probable regulatory mechanisms. Limnol. Oceanogr. **16:** 387–404.

NIXON, S. W. 1981. Remineralization and nutrient cycling in coastal marine ecosystems, p. 111–138. *In* B. W. Nelson and L. E. Cronin [ed.], Nutrient enrichment in estuaries. Hermana.

RAISWELL, R. 1993. Kinetic controls on depth variations in localised pyrite formation. Chem. Geol. **107:** 467–469.

REEBURGH, W. S. 1967. An improved interstitial water sampler. Limnol. Oceanogr. **12:** 163–165.

RUTTENBERG, K. C. 1992. Development of a sequential extraction method for different forms of phosphorus in marine sediments. Limnol. Oceanogr. **37:** 1460–1482.

———, AND R. A. BERNER. 1993. Authigenic apatite formation and burial in sediments from non-upwelling, continental margin environments. Geochim. Cosmochim. Acta **57:** 991–1007.

RUZIKA, J., AND E. H. HANSEN. 1980. Flow injection analysis. Wiley Interscience.

SCHOONEN, M. M. A., AND H. L. BARNES. 1991. Reactions forming pyrite and marcasite from solution. II. Via FeS precursors below 100°C. Geochim. Cosmochim. Acta **55:** 1505–1514.

SCHWERTMANN, U., AND E. MURAD. 1983. Effect of pH on the formation of goethite and hematite from ferrihydrite. Clays Clay Min. **31:** 277–284.

SIGG, L., AND W. STUMM. 1980. The interactions of anions and weak acids with the hydrous goethite (a-FeOOH) surface. Coll. Surf. **2:** 101–107.

SILVERBERG, N., AND OTHERS. 1986. Radionuclide profiles, sedimentation rates, and bioturbation in modern sediments of the Laurentian Trough, Gulf of St. Lawrence, Oceanol. Acta **9:** 285–290.

STURGEON, R. E., J. A. H. DESAULNIERS, S. S. BERMAN, AND D. S. RUSSEL. 1982. Determination of trace metals in estuarine sediments by graphite-furnace atomic absorption spectrometry. Anal. Chim. Acta **134:** 283–291.

SUNDBY, B., C. GOBEIL, N. SILVERBERG, AND A. MUCCI. 1992. The phosphorus cycle in coastal marine sediments. Limnol. Oceanogr. **37:** 1129–1145.

VAN CAPPELEN, P., AND E. D. INGALL. 1996. Redox stabilization of the atmosphere and oceans by phosphorus-limited marine productivity. Science **271:** 493–496.

WAYCHUNAS, G. A., B. A. REA, C. C. FULLER, AND J. A. DAVIS. 1994. Surface chemistry of ferrihydrite. 1. EXAFS studies of the geometry of coprecipitated and adsorbed arsenate. Geochim. Cosmochim. Acta **57:** 2251–2269.

YEATS, P. A. 1988. Nutrients, p. 1–15. *In* Chemical Oceanography in the Gulf of St. Lawrence. Can. Bull. Fish. Aquat. Sci. 220.

ZHAO, J., F. E. HUGGINS, Z. FENG, AND G. P. HUFFMAN. 1994. Ferrihydrite: Surface structure and its effect on phase transformation. Clays Clay Min. **42:** 737–746.

Received: 20 May 1996
Accepted: 30 April 1997
Amended: 19 June 1997